Clustering of Au on the faulted half of the Si(111)-7×7 unit cell

S. K. Ghose,[1] P. A. Bennett,[2] and I. K. Robinson[1]
[1]*Department of Physics, University of Illinois, Urbana, Illinois 61801, USA*
[2]*Department of Physics and Astronomy, Arizona State University, Tempe, Arizona 85287, USA*
(Received 28 December 2004; published 18 February 2005)

We present a structure for Au deposited on the Si(111)-7×7 surface at very low coverage obtained by x-ray diffraction. We have found Au adsorbed exclusively on the faulted side of the Si(111)-7×7 unit cell. The Au atoms are found to reside in sites which lie above the Si and do not cause significant rearrangement of the covalent bonding network of the substrate, suggesting they are weakly bound. The sites have considerable disorder and can be modeled by a strongly anisotropic Debye-Waller factor. From this we extract the potential for interaction of Au with Si(111) 7×7, which is in reasonable agreement with theoretical predictions for Si and other species on Si(111) 7×7.

DOI: 10.1103/PhysRevB.71.073407 PACS number(s): 68.43.Fg, 61.10.Eq, 61.46.+w, 81.07.−b

Self-organization in strained homoepitaxial thin-film growth[1,2] and self-assembly during chemical synthesis[3] are two of the most commonly used methods to obtain ordered metal nanostructures. Here we explore a third option, the use of a well-ordered surface as a nanoscale template.

The structure of 7×7 reconstruction of Si(111) surface is notable for its high stability and its relatively large unit-cell size, which makes it attractive for the exploration of template-based nanoscale self-assembled materials. The dimer-adatom stacking-fault (DAS) model[4] has alternations of triangular regions with faulted stacking between the third and fourth layers, joined by dimers along the edges and decorated on top with a locally 2×2 array of "adatoms." The structure is stabilized by reducing the number of "dangling" bonds from 49 to 19 per unit cell. These are located at 12 adatoms per unit cell, which have an unusual back-bonding geometry, at six "rest" atoms and at the bottom of a corner hole.[5]

Self-assembled growth of metal nanostructures on the Si(111)-7×7 surface has been extensively studied under a wide range of different conditions.[6–11] The specific case of Au on Si(111) 7×7 has been found for low as well as high coverage to show new reconstructed phases like 5×2, $\sqrt{3}\times\sqrt{3}$, and 6×6.[12] These structures become possible through chemical reaction of Au with Si. The Si(111)-7×7 structure is relatively inert to chemical reaction because of its tightly bonded electronic configuration. Upon deposition of Au on Si(111) 7×7, relatively high annealing temperatures or relatively high coverage are required to cause reaction either to silicides or these surface structures of new periodicity. By omitting this annealing step and using low coverage it is therefore possible to create metastable adsorbed states on the unperturbed substrate. The metastable state exists whenever the metal atoms have insufficient activation energy to enter the chemisorbed state, which would lead to the new reconstructions mentioned above. Such "soft" preparation conditions have been demonstrated with STM measurements for different metals to form nanoclusters on Si(111) 7×7, keeping the 7×7 symmetry and its inherent long-range order intact.[6,11] Especially on semiconductor surfaces, STM is strongly influenced by electronic structure as well as physical structure. For definitive atomic structure, a method sensitive to the locations of the atomic cores, such as surface x-ray diffraction (SXRD) is preferable.

Metastable perturbation structures are attractive for theoretical study because they do not require the evaluation of large numbers of hypothetical structures. Fortunately, the salient features of the surface, the adatoms and rest atoms, can be abstracted into a 4×4 unit cell that greatly facilitates the total energy calculations for a large unit cell like Si(111) 7×7. This was done by Cho and Kaxiras,[13,14] who found there were *basins of attraction* where adsorbed atoms attached to the surface. Surprisingly, the minima of potential were located away from the dangling bonds on the adatoms and rest atoms, which naively would be thought to be favorable for bond formation.

Here we report the structure of a low coverage of Au on Si(111) 7×7 at room temperature obtained by surface x-ray diffraction. X rays are particularly sensitive to high-Z Au atoms, which turns out to be important to counteract the large amount of disorder associated with the metastable state. Using difference Fourier methods, we find a structure with Au bound exclusively to the faulted side of Si(111)-7×7 unit cell close to the B_2 site predicted by Cho and Kaxiras.[14] Refinement of the structure with high-resolution data permitted a full anisotropic Debye-Waller factor (DWF) to be measured, which can be related to the interaction potential of the Au with the surface. The derived potential is in reasonable agreement with the theory and invites further theoretical study for Au on a finer grid.

Our experiments were performed at beamline X16A of the National Synchrotron Light Source (NSLS).[15] Bending magnet radiation was monochromated to $\lambda = 1.296$ Å using double Si(111) crystals. The sample was aligned by means of bulk Bragg reflections using a hexagonal coordinate system in which the Miller index L runs perpendicular to the surface plane. Clean Si(111)-7×7 surfaces were prepared in UHV chamber at a pressure of about 10^{-10} Torr, from Si wafers rinsed in alcohol, degassed at 500 °C, and flashed to 1200 °C followed by standard annealing procedure. The surface quality was examined by low-energy electron diffraction (LEED) and also by monitoring the in-plane $(\frac{3}{7},0)$ and $(1,\frac{3}{7})$ reflection peaks of the 7×7 reconstruction. The in-plane (L

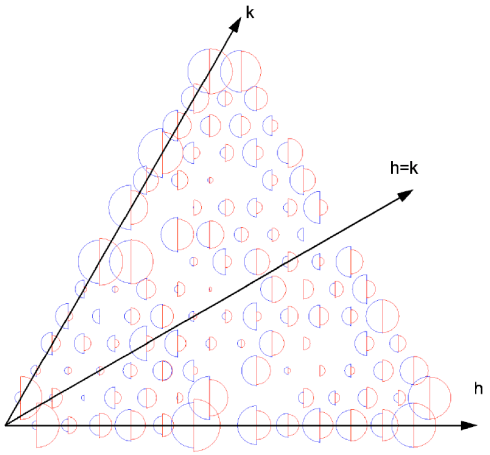

FIG. 1. (Color online) Out-of-plane ($L=1.5$) x-ray diffraction measurements of structure factors on the Si(111)-7×7 surface. Asymmetric unit cell for $p3m1$ symmetry shows the observed structure factors for clean (left half circles) and for low coverage (0.06 ML) Au (right half circles). The radius of each circle is proportional to the amplitude, the area to intensity. Broken symmetry is observable about the $h=k$ line for Au on Si data, but not with the clean data.

$=0.25$) and out-of-plane ($L=1.5$) data were measured for the 7×7 clean surface before gold deposition. Gold was then evaporated from a coated tungsten filament onto the sample held at room temperature at a deposition rate of 0.03 monolayers (MLs)/min. The coverage was determined from the calibration curve obtained from the measurement of deposition time and thickness with respect to different known Au-Si reconstructed stuctures ($5\times2, \sqrt{3}\times\sqrt{3}$, and mixed stuctures) while monitoring the LEED pattern and a few x-ray reflections. The error estimated on Au coverage, based on the limitations of quartz balance, LEED, and x-ray measurements, is approximately 10%. Measurements are made for coverage ranges from 0.06 to 0.18 MLs. To extract the structure, factors quantitatively, the intensities were integrated over orientation angle ϕ, background subtracted, and corrected for the Lorentz factor, polarization, and active sample area.[16] The structure factors were averaged with $p3m1$ and $p6mm$ surface-group symmetries separately and corresponding nonequivalent structure factors were used for fitting to the model.

A striking feature of the DAS model[4] of Si(111) 7×7 is that the surface has *higher* symmetry than the bulk. There is an extra mirror line which separates the two halves of the 7×7 unit cell into a faulted and unfaulted halves, depending on whether or not a stacking fault exists between the third and fourth layers. This mirror raises the surface symmetry to $p6mm$ from $p3m1$ in the bulk. This difference in symmetry can be easily detected in reciprocal space. Surface x-ray diffraction is sensitive to this symmetry difference for measurements taken out of plane, i.e., when the perpendicular momentum transfer is nonzero, in our case for $L=1.5$. Figure 1 shows the measured structure factors (SFs) of the $L=1.5$ reciprocal-lattice section for both the clean and gold covered surfaces, showing a distinct pattern. The mirror line in question corresponds to the $h=k$ line in reciprocal space. It is clear that the clean data are symmetric about $h=k$ while the gold-covered data break this symmetry.

TABLE I. Values of reproducibility factor (ϵ) among different symmetry equivalent reflections obtained from averaging structure factor data with $p6mm$ and $p3m1$ symmetry for $L=1.5$ data. The number in the parentheses represent the number of strong reflections used to determine the agreement factor.

Data set	$p6mm$	$p3m1$
Clean	0.080(33)	0.060(30)
0.06ML	0.155(30)	0.079(25)
0.12ML	0.110(30)	0.053(30)
0.18ML	0.079(23)	0.052(20)

For each coverage, we have measured 199 structure factors for each in-plane ($L=0.25$) and out-of-plane ($L=1.5$) data set. This yields 57 nonequivalent reflections averaging with $p6mm$ symmetry and 107 nonequivalent reflections with $p3m1$ symmetry. The reproducibility factor (ϵ) is the *mean normalized standard deviation* of the measured structure factors,[16] which signifies the agreement with the symmetry. Values of ϵ for both symmetries as a function of coverage are listed in Table I. It is observed that for lower coverage (0.06 ML) gold data, ϵ with $p6mm$ symmetry average is about double the value compared to that of clean data. This is a strong evidence that the low coverage Au data set has broken the $p6mm$ symmetry.

The interpretation of crystallographic data is limited by the inability to measure the phase of the complex SF. To avoid the inherent "phase problem," we employ the *difference Fourier* (DF) method,[17] which has been applied before to surface problems.[16] We analyzed the lowest coverage (0.06 ML) data using the known clean surface as a reference structure. Figure 2 shows a contour plot of three-dimensional (3D) difference map at $z=2$ Å, which is approximately the Si

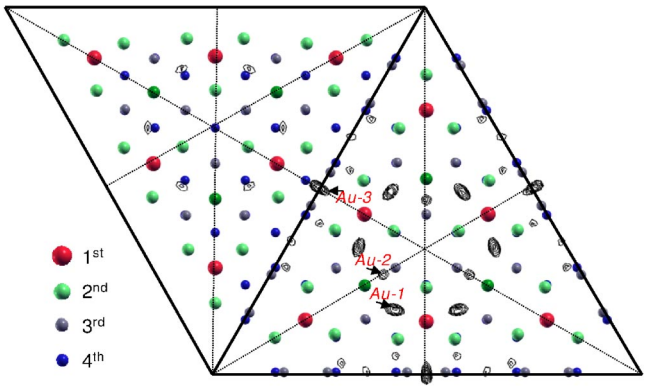

FIG. 2. (Color online) 3D difference Fourier map between clean (calculated) and low coverage (0.06 ML) Au (observed) on the Si(111)-7×7 surface. Equally spaced positive contours are drawn within the 7×7 unit cell. The DAS model (Ref. 4) is overlayed for reference. The faulted half of the unit cell is to the lower right side of the mirror line (short diagonal) passing through the dimer rows. Dotted lines are the mirror lines on the surface. Peaks are labeled as Au-1, Au-2, and Au-3 and define three candidate sites of Au adsorption.

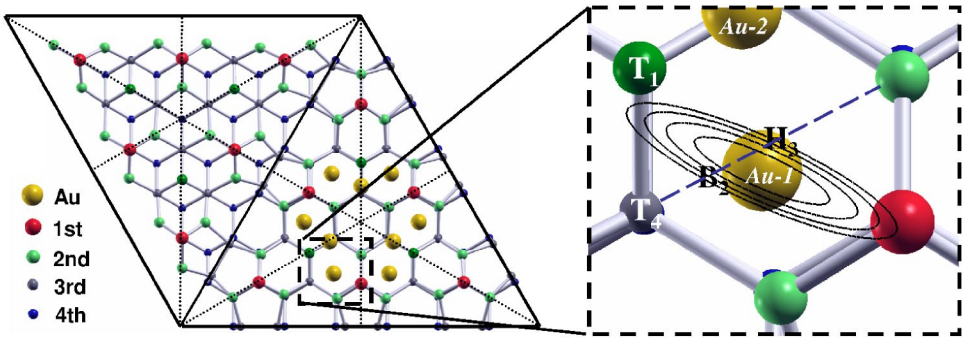

FIG. 3. (Color online) Top view of the model for the structure of an Au nanocluster on the faulted side of the Si(111)-7×7 surface. Six of the nine Au atoms (Au-1) reside within the *basins of attraction* and the other three Au atoms (Au-2) are lying on the symmetry lines (dotted) near to the rest atoms (T_1). Equipotential contours derived from Eq. (1) are drawn for 50-, 100-, 150-, and 200-meV energy levels. The labels H_3, B_2, T_1, and T_4 are the sites where CK have calculated the potential (Ref. 14)

adatom height. The DAS model is superimposed to visualize the positions of the extra peaks with respect to the clean surface. The map clearly shows that the positive differences, suggesting the location of the Au atoms, fall exclusively on the faulted side of the unit cell. The preferential adsorption of Au atoms on the faulted half of the unit cell at low coverage is in agreement with previous results reported for different metals by STM experiments[6–11] which are sensitive to this features. The preference is presumed to be due to an adsorption energy difference between the two sides, reported to be in the range 0.05-0.1 eV.[11,18,6]

The DF map suggests three positions of Au binding sites within the unit cell. These positions are denoted Au-1(6×), Au-2(3×), and Au-3(3×). The latter two sites lie on mirror lines of *p*3*m*1 so are only threefold degenerate. Hence the unit cell consists of nine Au atom peaks at the center of the faulted half of the unit cell and three peaks at the center of the dimer rows. Models were built with different combination of these Au-adatom arrangements and tested against the data using "ROD" least-squares analysis program.[19]

Experimental in-plane diffraction data for the clean surface were first fitted to fine tune the DAS model. The least-squares fit to the clean in-plane data with refinement of 15 parameters for the displacement of positions consistent with *p*6*mm* symmetry and Debye-Waller parameters gave a χ^2 value of 1.87 and refined positions which compare well with those obtained previously.[20] To obtain the out-of-plane *z* coordinate information fit the $L=0.25$ and $L=1.5$ data, varying *z* position of top three layers of the DAS model, keeping all other parameters fixed and still maintaining *p*6*mm* symmetry. We obtained a best fit with χ^2 value of 3.5. The higher χ^2 values can be attributed to the lower accuracy of the out-of-plane data.

We then made a 3D fit to 214 *p*3*m*1-averaged structure factors for gold data varying the Au positions and occupancies parameters. In our model we first considered all the three positions (Au-1, Au-2, and Au-3) of the Au per asymmetric section of the unit cell. We kept the Si positions fixed at the clean DAS positions and varied only parameters linked to the *z* position and occupancy of Au atoms. The clean model without Au atoms gave a χ^2 value of 16. Refinement with Au at all the three positions as of the DF map (see Fig. 2) gave a χ^2 value of 4.5. We obtained the occupancy values for Au-1 and Au-2 as 0.15 and 0.14, respectively but the gold at Au-3 positions had zero occupancy. The occupancy being less than the coverage is believed to arise from absence of the clusters in some of the unit cells. The elongated shape of the positive peaks at Au-1 positions in the 3D difference map (Fig. 2) suggests anisotropic Debye-Waller factors (DWFs) for those Au atoms. Refinement of this structure drops the χ^2 value to 3.95 which we accept as the best fit with the model shown in Fig. 3. The *x*, *y* positions (in fractional co-ordinate of the unit cell) of the Au-1 and Au-2 atoms in the asymmetric section of the faulted half of the 7×7 unit cell are 0.5077 ± 0.0014, 0.1708 ± 0.0018 and 0.548 ± 0.002, 0.274 ± 0.002, respectively. We obtained values of the anisotropic DWFs for the Au-1 atom present in the asymmetric section unit cell are $B_{11}=9.247\pm1.109$, $B_{22}=5.215\pm0.938$, $B_{12}=-5.017\pm1.015$ and the isotropic DWF for the Au-2 atom in the same section is $B=2.845\pm0.293$. The DWFs are the thermal parameters in the same unit as the conventional isotropic thermal parameters *B*.[21–23]

Figure 3 also shows the location and names of the atomic sites tested in the theoretical study of Cho and Kaxiras.[14] The rest atom site (T_1) is surrounded by a *basin of attraction* containing the H_3, B_2, and T_4 sites. In most cases, the potential minimum for Si, Ge, Mg, K interaction with Si(111) 7×7 occurs at the low-symmetry "B_2" site, roughly equidistant from the adatoms and rest atoms. In our model (Fig. 3) the Au-1 site is close to this B_2 site. The anisotropic DWF measured for Au-1 atoms can be considered to be due to motion of the weakly bound Au atom in an effective interaction potential of Au with the Si surface. We can derive the harmonic potential from the anisotropic DWF using the relation.[21,22]

$$V(x,y) = -k_B T \ln[\rho(x,y)], \tag{1}$$

where k_B is Boltzmann's constant, T is temperature, and $\rho(x,y)$ is the Gaussian probability density function whose Fourier transform was used to fit the data. The potential contours shown in Fig. 3, suggests the Au-1 atom has freedom to move around in the hexagonal pocket while avoiding the dangling bond sites (Si-rest atom and Si adatom). Figure 4 shows a comparison between the site dependent binding energies calculated by Cho and Kaxiras (CK) for Si and the

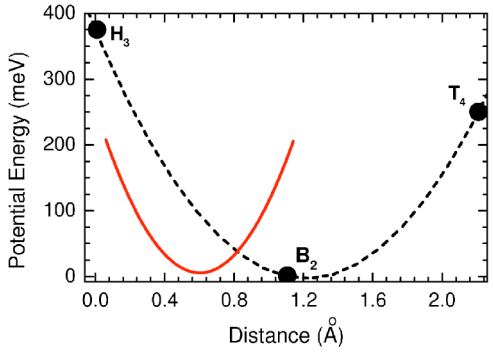

FIG. 4. (Color online) Comparison of the potential calculated by CK for Si on the Si(111)-7×7 surface (dashed line) and measured potential for Au-1 (solid line). The points H_3, B_2, and T_4 are the sites where the potential was evaluated by CK (Ref. 14). Potentials were measured along the line (dashed line in Fig. 3) connecting H_3, B_2, and T_4 points.

potential derived from our measurement for Au atoms on Si(111) 7×7. The derived potential is in reasonable agreement with the theory for Si adsorption on Si(111) 7×7 given by CK, considering that Au and Si atoms should bind differently and that CK's potential interpolates three calculated values.

The three Au-2 atoms can be explained by the Au-Au interactions that lead to nanocluster formation. It is known that other metals have a tendency to agglomerate to form dimers and trimers on Si.[8] This tendency of metals have been addressed explicitly for Pb-Pb interaction on the Si(111) -7×7 surface by Sonnet *et al.*[18] In our case the Au-2 sites could be the result of Au-Au interaction between Au-1 and Au-2, as evident from Au-1-Au-2 bond lengths of 2.68±0.3 Å. The Au-1 atoms are 1.0±0.3 Å higher than the Si-adatom position, while the three Au-2 atoms are about 0.4±0.3 Å lower than the Au-1 atoms. The Au-Si bond lengths for Si-rest atom and Si-adatom are 2.96±0.3 Å and 2.48±0.3 Å, respectively, which is more than the usual Au-Si bond length. It is noteworthy that the Au-1 atoms are bound far away from the dangling bonds of the Si-rest atom and Si adatom. The closest distance in the structure is the Au-2 atom which is 2.14±0.3 Å from the Si-rest atom.

A closer observation to Table I tells us that the *p*6*mm* symmetry of the surface is broken for low coverages (0.06 and 0.12 ML) but that the higher symmetry is restored for the higher coverage (0.18 ML). Further DF studies (not shown) indicate that for 0.12 ML the occupancy of Au atoms increases but they are still within the *basin of attraction* sites on the faulted half of the unit cell, whereas for the 0.18-ML coverage Au becomes adsorbed on both halves of the unit cell and at the corner hole of the unit cell. This causes the restoration of the surface symmetry to *p*6*mm* for the Si(111)-7×7 surface.

In summary, we have observed by surface x-ray diffraction the formation of nanoclusters of Au on the Si(111)-7×7 surface. At a very low coverage and room-temperature Au was found to adsorb at the faulted halves of the unit cell. One binding site was disordered, suggesting a range of positions within a broad potential minimum. The second site is at a reasonable contact distance from the first. Combining these two sites, a metastable Au cluster of nanometer size is formed. The potential derived from our model agrees quite well with the DFT calculation made by Cho and Kaxiras[13,14] for different species on the Si(111)-7×7 surface.

This work was supported by Air Force Office of Scientific Research MURI Grant No. F49620-01-1-0336. The X16A beam line is supported by the DOE under Grant No. DEFG02-91ER45439 and NSLS is supported by DOE under Grant No. DEAC02-98CH10886.

[1] H. Brune, M. Giovannini, K. Bromann, and K. Kern, Nature (London) **394**, 451 (1998).
[2] K. Bromann, C. Félix, H. Brune, W. Harbich, R. Monot, J. Buttet, and K. Kern, Science **274**, 956 (1996).
[3] S. Sun, C. B. Murray, D. Weller, L. Folks, and A. Moser, Science **287**, 1989 (2000).
[4] K. Takayanagi, Y. Tanishiro, S. Takahasi, M. M. Takahasi, Surf. Sci. **164**, 367 (1985).
[5] D. Vanderbilt, Phys. Rev. Lett. **59**, 1456 (1987).
[6] Jian-Long Li, J-F. Jia, X-J. Liang, Xi Liu, J-Z. Wang, Q-K. Xue, Z-Q. Li, J. S. Tse, Z. Zhang, and S. B. Zhang, Phys. Rev. Lett. **88**, 066101 (2002).
[7] E. Ganz, F. Xiong, I-S. Hwang, and J. Golovchenko, Phys. Rev. B **43**, 7316 (1991).
[8] J. M. Gómez-Rodríguez, J. J. Sáenz, A. M. Baro, J-Y. Veuillen, and R. C. Cinti, Phys. Rev. Lett. **76**, 799 (1996).
[9] S. Tosch and H. Neddermeyer, Phys. Rev. Lett. **61**, 349 (1988).
[10] M. Yoon, X. F. Lin, I. Chizhov, H. Mai, and R. F. Willis, Phys. Rev. B **64**, 085321 (2001).
[11] L. Vitali, M. G. Ramsey, and F. P. Netzer, Phys. Rev. Lett. **83**, 316 (1999).
[12] D. Grozea, E. Bengu, and L. D. Marks, Surf. Sci. **461**, 23 (2000), and references therein.
[13] K. Cho and E. Kaxiras, Europhys. Lett. **39**, 287 (1997).
[14] K. Cho and E. Kaxiras, Surf. Sci. **396**, L261 (1998).
[15] P. H. Fuoss and I. K. Robinson, Nucl. Instrum. Methods Phys. Res. A **222**, 171 (1984).
[16] I. K. Robinson, in *Handbook of Synchrotron Radiation*, edited by D. E. Moncton and G. S. Brown (North-Holland, Amsterdam, 1986), Vol. 3.
[17] W. Cochran, Acta Crystallogr. **4**, 408 (1951).
[18] Ph Sonnet, L. Stauffer, and C. Minot, Surf. Sci. **407**, 121 (1998).
[19] E. Vlieg, J. Appl. Crystallogr. **33**, 401 (2000).
[20] I. K. Robinson, W. K. Waskiewicz, P. H. Fuoss, and L. J. Norton, Phys. Rev. B **37**, 4325 (1988).
[21] H. L. Meyerheim, I. K. Robinson and R. Schuster, Surf. Sci. **370**, 268 (1997).
[22] W. F. Kuhs, Acta Crystallogr., Sect. A: Found. Crystallogr. **48**, 80 (1992).
[23] G. H. Stout and L. H. Jensen, *X-ray Structural Determination, A Practical Guide* (Wiley, New York, 1989).